iScience

CellPress
OPEN ACCESS

Article

Cultural and demic co-diffusion of Tubo Empire on Tibetan Plateau

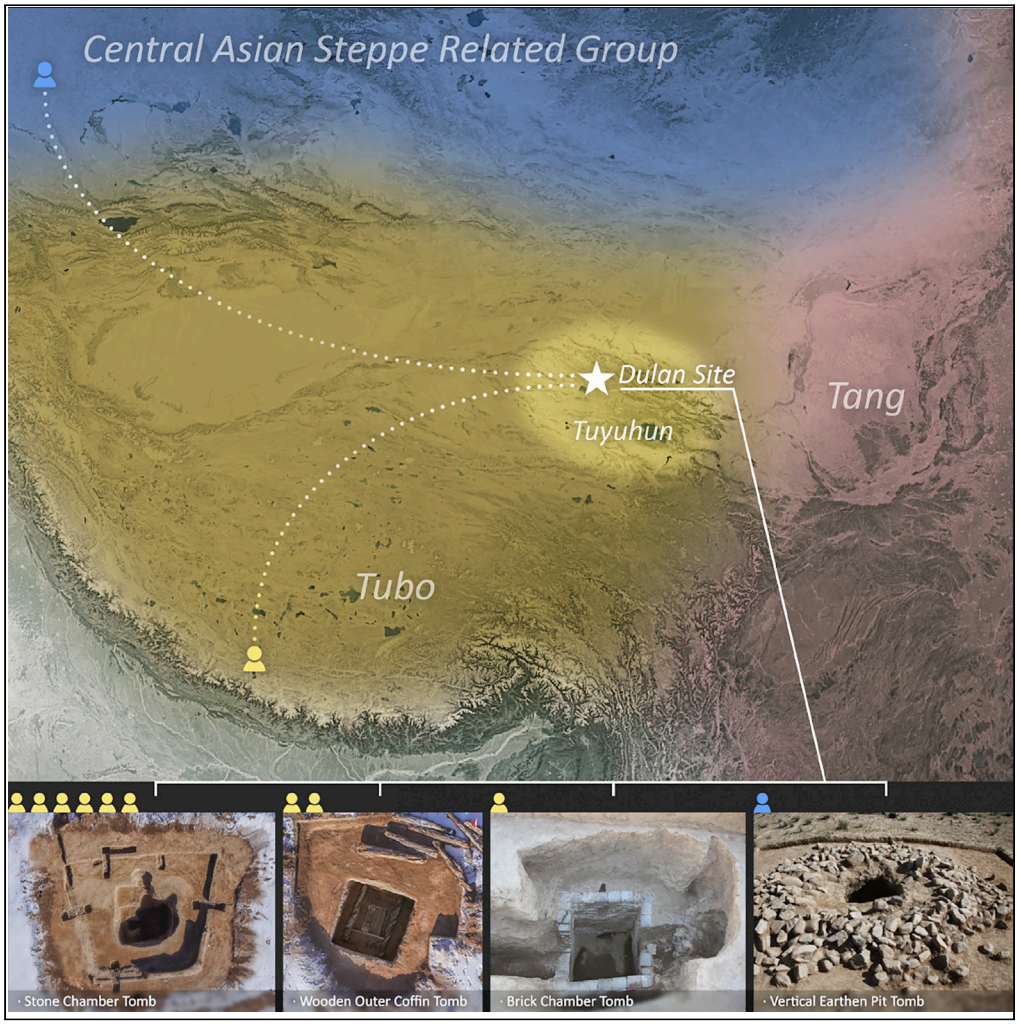

Kongyang Zhu, Panxin Du, Jiyuan Li, ..., Guanghui Dong, Chuan-Chao Wang, Shaoqing Wen

wang@xmu.edu.cn (C.-C.W.)
wenshaoqing@fudan.edu.cn (S.W.)

Highlights

The cultural and demic co-diffusion of Tubo Empire on Tibetan Plateau

Potential population movement into the Tubo-controlled regions from Central Asia

Zhu et al., iScience 25, 105636
December 22, 2022
https://doi.org/10.1016/j.isci.2022.105636

iScience

CellPress
OPEN ACCESS

Article

Cultural and demic co-diffusion of Tubo Empire on Tibetan Plateau

Kongyang Zhu,[1,2,15] Panxin Du,[3,4,15] Jiyuan Li,[5,15] Jianlin Zhang,[6] Xiaojun Hu,[5] Hailiang Meng,[3] Liang Chen,[7] Boyan Zhou,[8] Xiaomin Yang,[9] Jianxue Xiong,[1] Edward Allen,[1] Xiaoying Ren,[1] Yi Ding,[1] Yiran Xu,[1] Xin Chang,[1] Yao Yu,[1] Sheng Han,[3] Guanghui Dong,[10] Chuan-Chao Wang,[2,3,9,11,12,*] and Shaoqing Wen[1,3,13,14,16,*]

SUMMARY

A high point of Tibetan Plateau (TP) civilization, the expansive Tubo Empire (618–842 AD) wielded great influence across ancient western China. However, whether the Tubo expansion was cultural or demic remains unclear due to sparse ancient DNA sampling. Here, we reported ten ancient genomes at 0.017- to 0.867-fold coverages from the Dulan site with typical Tubo archaeological culture dating to 1308–1130 BP. Nine individuals from three different grave types have close relationship with previously reported ancient highlanders from the south-western Himalayas and modern core-Tibetan populations. A Dulan-related Tubo ancestry contributed overwhelmingly (95%–100%) to the formation of modern Tibetans. A genetic outlier with dominant Eurasian steppe-related ancestry suggesting a potential population movement into the Tubo-controlled regions from Central Asia. Together with archeological evidence from burial styles and customs, our study suggested the impact of the Tubo empire on the northeast edge of the TP involved both cultural and demic diffusion.

INTRODUCTION

As the world's largest and highest plateau, with an extreme environment making it one of the last major areas conquered by man,[1] the Tibetan Plateau (TP) has been the focus of numerous, often multidisciplinary studies aimed at elucidating the history of its human colonization. Multidisciplinary evidence has given us new clues about the prehistory of TP populations. The first is the "first arrival of humans at TP" scenario. The earliest archaic human remains, a Denisovan-like mandible found at the Baishiya Karst Cave site (3,280 meters above sea level [masl]) on the northeast edge of the plateau, suggest the presence of a Denisovan-related population on TP as early as 160 thousand years ago (kya).[2,3] The Nwya Devu site (4,600 masl) represents the earliest activities of anatomically modern humans on the TP, traceable to the most recent date of 30 kya.[4] Followed by the "settled permanently of humans on TP" scenario, one key factor which would enable modern humans to make a lasting home on the plateau was the ability to obtain sufficient survival materials. Combining travel cost modeling with archaeological data from the Chusang site,[5] Meyer et al. proposed that Chusang represents the earliest evidence of permanent settlement of modern humans on the TP known at present, dating to at least 7.4 kya.[6] Meanwhile, Chen et al. have argued that the emergence of a new agropastoral economy after 3.6 kya facilitated the durable, permanent settlement of modern humans on the TP.[7] Another critical factor for successful settlement on the plateau was an adaptation to the hypoxic environment.[8,9] Previous studies have shown that Tibetans possess unique endothelial PAS domain protein 1 (*EPAS1*) and HIF-1α prolyl hydroxylase1 (*EGLN1*) haplotypes, associated with adaptation to hypoxia.[10–14] It is believed that these unique haplotypes were introgressed into modern Tibetans from a Denisovan-like population, pointing to a separate admixture event between the upper Paleolithic inhabitants on the TP and later immigration of an upper Yellow River farming population.[15] This hypothesis is supported by several studies on uniparental markers[9,16–18] and analysis of genome-wide data.[19]

By comparison with research on prehistoric TP populations, the population history of the historical TP has been relatively limited. The Tubo empire stands out as a period of particular interest. On the one hand, the Tubo empire was the first and only imperial regime on the TP. During the mid-7th century, more than a dozen ancient Tibetan tribes were united under the Bod tribe from the Yarlung Valley, located south of the plateau.[20] The Tubo empire was soon established with Luosuo (present-day Lhasa) as its capital,

[1]Institute of Archaeological Science, Fudan University, Shanghai 200433, China

[2]State Key Laboratory of Cellular Stress Biology, School of Life Sciences, Xiamen University, Xiamen 361102, China

[3]Ministry of Education Key Laboratory of Contemporary Anthropology, Department of Anthropology and Human Genetics, School of Life Sciences, Fudan University, Shanghai 200433, China

[4]State Key Laboratory of Genetic Engineering, Collaborative Innovation Center for Genetics and Development, School of Life Sciences, and Human Phenome Institute, Fudan University, Shanghai 200433, China

[5]Qinghai Provincial Cultural Relics and Archaeology Institute, Xining 810007, China

[6]Shaanxi Academy of Archaeology, Xi'an 710054, China

[7]China-Central Asia Human Environmental "the Belt and Road" Joint Laboratory, Northwest University, Xi'an 710127, China

[8]Division of Biostatistics, Department of Population Health, School of Medicine, New York University, New York, NY 10016, USA

[9]Department of Anthropology and Ethnology, Institute of Anthropology, School of Sociology and Anthropology, Xiamen University, Xiamen 361005, China

[10]Key Laboratory of Western China's Environmental Systems (Ministry of Education), College of Earth and Environmental Sciences, Lanzhou University, Lanzhou 730000, China

Continued

from which the empire would be administered for more than 200 years. Tubo territory reached its maximum extent from the end of the 8th through 9th centuries, stretching west from the Congling (葱岭, the Pamirs) bordering the Abbasids, east to present-day Longshan in Gansu Province and the western rim of the Sichuan Basin, north to Juyan Lake Basin (居延海), south to the border of Shindhu (天竺, i.e. Indian subcontinent). The Tubo was also a crucial period in the formation of modern Tibetan culture and identity, profoundly impacting the ethnolinguistic distribution of modern populations on the TP and surrounding areas.[21] In the case of Amdo Tibetan, classified as a dialect of Tibetan, its formation seems to have been precipitated by massive population migrations in the Amdo region (Gansu, Qinghai, and pastoral regions in northern Tibet), following a series of Tubo military conquests.[20,22] Tubo people integrated with local ethnic groups and gradually formed an Amdo Tibetan identity and language.[21]

The Tubo rise and expansion affected the course of history across eastern Eurasia, but the genetic impact of its cultural and military expansion is poorly understood. On the southwest edge of the TP, two studies reported individuals from Himalayan sites in Mustang and Manang districts,[23,24] providing the earliest genetic profiles of the TP population, dating to at least 1317 BCE. Both studies revealed close genetic connections between ancient Himalayan populations and modern Tibetans. A separate study analyzing 60 genomes for four modern populations from Pakistan and Tajikistan suggested that the impact of the Tubo empire on Baltistan involved dominant cultural and minor demic diffusion.[25]

Dulan district was a major hub of the Qinghai route along the ancient Silk Road. Numerical surveys discuss the presence of thousands of Tubo-style tombs in the Dulan district, making this the most concentrated region of Tubo-related burials on the northern TP. A recent study reported the genetic data of eight Dulan individuals, but only three individuals were used to perform genomic analysis while the others were excluded due to high contamination or insufficient data. However, the coverages of those three used individuals were quite low with only <85k SNPs overlapping with the 1240k dataset, which hindered the close inspection of Dulan populations.[26] In this study, we sampled ten ancient individuals from the Dulan Wayan reservoir site (3180 masl), located around 2 km southeast of the Zamari village in Reshui town, Dulan county (hereafter called the Dulan site) (Figure 1). Tombs were classifiable into four groups according to discernible grave typologies: stone chamber tomb, wooden outer coffin tomb, earthen pit tomb, and brick chamber tomb. Overall, based on burial style and custom, such as the most common stone chamber tombs with trapezoidal floor plan, unearthed objects with ink writings in Tibetan, and intact horses in strip-shaped sacrificial pits, the Dulan site exhibits typical Tubo-style burial characteristics. Furthermore, radiocarbon dating methods were used to date all samples (Tables 1 and S1). With the exception of one outlier value, dated 1308 BP, the remaining samples fell into the 1232–1130 BP range, i.e., in the aftermath of the Tuyuhun (a polity established by nomadic-pastoral Xianbei peoples from northeast China) defeat and annexation by Tubo, occurring at 663 AD (i.e., 1287 BP). Both archaeological culture and radiocarbon dating supported Dulan's Tubo ascription, meaning excavated remains presented an outstanding opportunity to study the expansion of the Tubo empire on the northeast edge of the TP.

RESULTS

Ancient genome-wide data from the Dulan site

In this study, we generated genome-wide data from 10 ancient samples from the Dulan site with 0.017- to 0.867-fold coverage (Tables 1 and S1). These represent the ancient genome-wide data from the Ganqing region dated to the Tubo Empire period. Samples were filtered through several preliminary steps. We first verified the authenticity of genome-wide data by identifying the presence of characteristic postmortem patterns of ancient DNA (Figure S1).[27] Second, we estimated the degree of kinship between samples using lcMLkin, detecting no close relationship (under second degree) (Table S1).[28] Third, we assessed the modern human contamination using mitochondrial- and autosomal-based methods: the evidence appointed to a low level of modern human contamination, <3% for mtDNA for all samples and <3% nuclear contamination for all males with a supported number of SNPs over 200 in angsd analysis (Table S1).[29,30] We then generated pseudo-haploid genotypes for each sample using a 1240k panel after trimming 4 bp at each end of the reads. As a result, we generated genotyping data of 10 individuals covering 21,411–682,505 SNPs in the 1240k panel. A sample with coverage lower than 50,000 SNPs (Individual ID: BB2012) was labeled "Dulan_LowCov" and used exclusively for individual-based analyses, including principal component analysis (PCA) and ADMIXTURE. We performed the pairwise-*qpWave* first to detect whether our samples belonged to a single homogenous group (Figure S2). One individual (Individual ID: BB2013) significantly differed from the others and was labeled "Dulan_o" in subsequent analysis, while other samples

[11]State Key Laboratory of Marine Environmental Science, Xiamen University, Xiamen 361102, China

[12]Institute of Artificial Intelligence, Xiamen University, Xiamen 361005, China

[13]MOE Laboratory for National Development and Intelligent Governance, Fudan University, Shanghai 200433, China

[14]Center for the Belt and Road Archaeology and Ancient Civilizations, Shanghai 200433, China

[15]These authors contributed equally

[16]Lead contact

*Correspondence: wang@xmu.edu.cn (C.-C.W.), wenshaoqing@fudan.edu.cn (S.W.)

https://doi.org/10.1016/j.isci.2022.105636

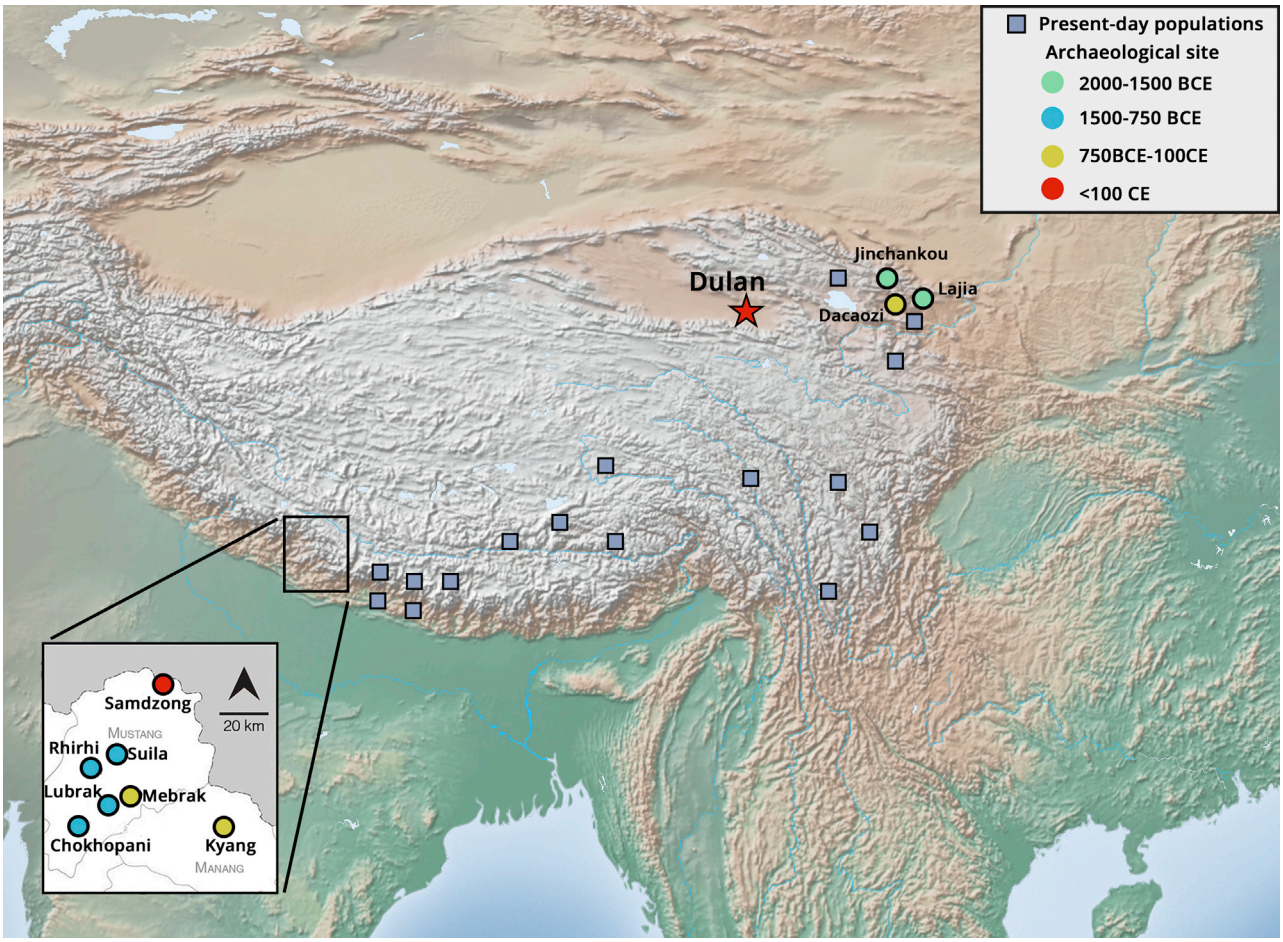

Figure 1. Geographic information of ancient individuals
Geographical location of newly sampled ancient Dulan samples.

formed a homogenous group at our current resolution and were collectively labeled "Dulan" (Tables 1 and S1). We then merged our data with published 1240k and Human Origin datasets (see STAR methods for further details).[15,23,31–38] The Human Origin dataset was used in analyses that involved modern populations, while the 1240k dataset was used in all other analyses.

Overall qualitative genomic structure shows the close relationship of Dulan to other high-altitude East Asian

Overall population structure was initially examined through a PCA (Figure 2).[39] The PCA result formed a triangle with Northeast Asian-related (NEA), Southeast Asian-related (SEA), and Tibetan-related modern populations at the three vertices. Ancient individuals from coastal and inland Southeast Asia clustered and projected in close proximity to SEA-related Ami and Atayal populations, ancient individuals from the Eurasian steppe were projected close to the cline formed by NEA-related Turkic- and Mongolic-speaking populations, and ancient individuals from Nepal (aMMD, ancient individuals from Mustang and Manang districts)[24] were projected close to the Tibetan-related populations reported by Wang et al.[34] Wang et al. observed that modern Tibetan populations could be divided into three genetic clusters: the core-Tibetan group, northern-Tibetan group exhibiting core-Tibetan and West Eurasian admixture, and a corridor-Tibetan group with a larger Southeast Asian component. We found that all Dulan individuals overlapped with aMMD. Dulan and aMMD were projected between the cline formed by the modern core-Tibetan populations and ancient individuals from the upper Yellow River region (Upper_YR_LN and Shimao_LN),[15] though showing nearer relation to the Tibetan-related side. Unlike the Dulan samples, Dulan_o is projected close to modern Turkic- and Mongolic-speaking populations and closest to ancient

Table 1. Summary of ancient samples reported in this study

Individual ID	Label	Data range[a] (cal.AD)	Sex	5p C->T	MT contamination	Coverage	num of SNPs (1240k)
BB2004	Dulan	708–884	F	4.53%	1.29%	0.048	53366
BB2005	Dulan	658–775	M	4.49%	0.81%	0.181	203837
BB2006	Dulan	706–883	F	5.58%	0.78%	0.215	219910
BB2007	Dulan	682–878	F	1.54%	0.98%	0.332	334369
BB2008	Dulan	670–775	F	8.40%	1.48%	0.110	123378
BB2009	Dulan	658–775	M	8.21%	0.47%	0.867	682505
BB2010	Dulan	667–774	M	4.73%	0.98%	0.239	247877
BB2011	Dulan	605–665	F	6.03%	0.32%	0.395	367122
BB2012	Dulan_LowCov	667–774	M	9.30%	2.22%	0.017	21411
BB2013	Dulan_o	670–798	M	3.64%	0.87%	0.150	168987

Data range reports the combination of time range from calibrated 14C dates and estimates from archeological contexts. See more details in Table S1.
[a]Combination of all calibrated ^{14}C dates (95.4% CI) for all individuals. Detail information is available in Table S1.

individuals Kyrgyzstan Turk and Kazakhstan_Kipchak2 as previously reported in the study by Damgaard et al.[35]

Next, we performed a model-based ADMIXTURE analysis (Figures S3 and S4). A minimum cross-validation error was observed at k = 4, and we observed an orange component maximized in SEA-related populations, a yellow component maximized in Tungusic- and Mongolic-speaking populations, a pink component maximized in Eurasian steppe populations, and a blue component maximized in aMMD.[24] We also noted that the ancestral composition among the Dulan group is closest to modern core-Tibetan populations and ancient upper Yellow River farmers from Jinchankou and Lajia sites (Qijia culture, Upper_YR_LN).[15] Dulan possesses more blue components than any other non-aMMD population, indicating the close relationship between Dulan and aMMD. A similar pattern could be observed in pairwise-*qpWave* and outgroup-f_3 analyses. When assessing the homogeneity between different populations with aMMD in pairwise-*qpWave* analysis, only the modern Tibetan, modern Nepalese, and Dulan populations could provide the results with $p > 0.05$ in rank0, while Dulan always has a larger p-value than other populations except for Sherpa (Figure S5). Outgroup-f_3 statistics in the form of f_3(X, Y; Mbuti), which calculates the shared genetic drift between X and Y, also suggest that modern core-Tibetan populations, Dulan, and aMMD were more closely inter-related than they were to other populations (Figure S6).

In general, we found a close relationship between Dulan and aMMD, revealing shared genetic profiles related to high-altitude populations in the TP and the Himalayas. This type of ancestry has been referred to as the "Tibetan" lineage in Liu et al.[24] and remained apposite in our study. The discovery of an outlier (Dulan_o) cluster with ancient individuals from the Eurasian steppe and modern Turkic- and Mongolic-speaking groups (Figures 2 and S3–S6) suggested a possible link between Dulan and Steppe nomadic populations during the Tubo period.

Close inspection of the genomic profiles within Dulan and high-altitude East Asian populations

In order to quantify the genomic difference between Dulan and other high-altitude East Asian populations, we performed the f_4-statistics in the form of f_4(Mbuti, reference; aMMD, Dulan). This would allow us to directly compare the genetic profiles of aMMD and Dulan, using a "reference" set that included 89 populations from various places (Figure 3A). It was shown that Dulan did not share significantly more alleles with ancient North Eurasian (ANE), Eurasian Steppe, or South Asian groups, but shared an excess genetic affinity with the ancient North Asian (ANA) group when compared to aMMD (Table S2). Interestingly, Dulan showed the strongest genetic affinity with Lubrak compared to other populations from aMMD, i.e., with a Z-score of f_4(Mbuti, reference; Lubrak, Dulan) ranging from $-1.89<Z<2.91$. Liu et al.[24] considered Lubrak the earliest known representative population of the "Tibetan" lineage. We then performed the f_4-statistics in the form of f_4(Mbuti, reference; Tibetan, Dulan) to investigate the relationship between Dulan and modern Tibetan populations, where a "reference" set of 103 populations from various places and "Tibetan" groups included 11 modern Tibetan populations were used (Figure 3B). Our study was able to confirm

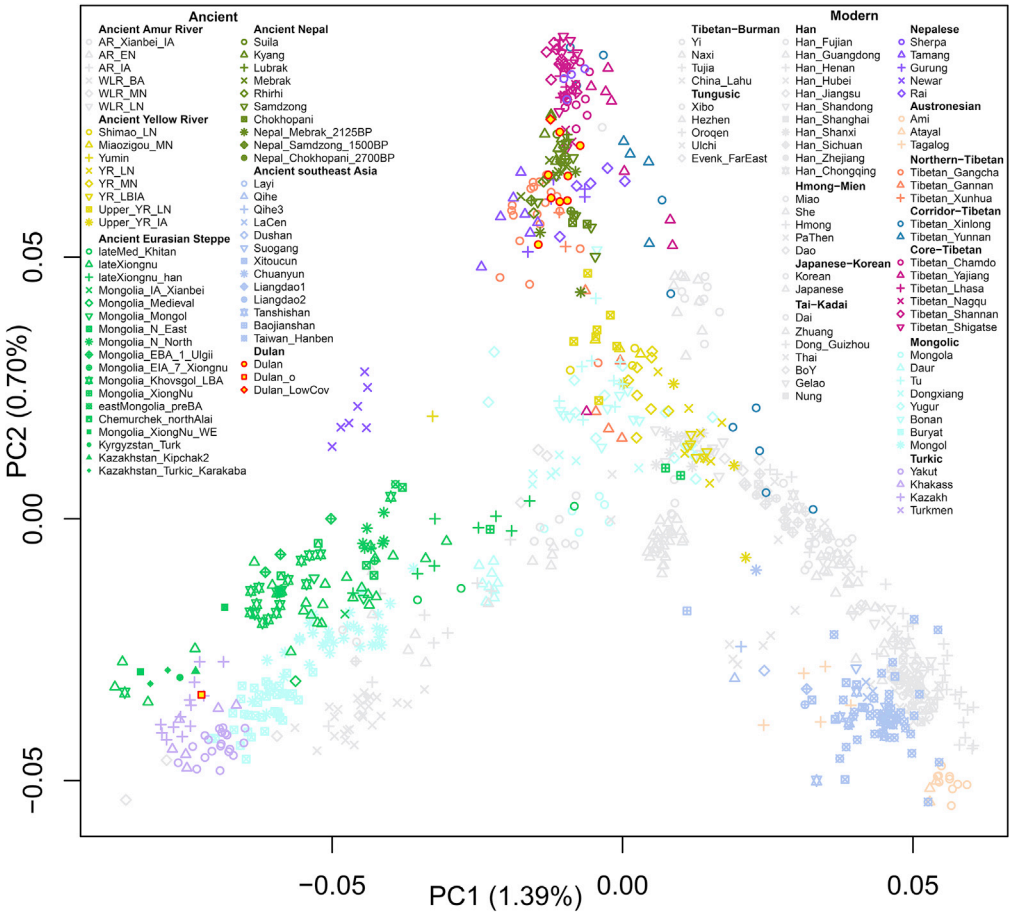

Figure 2. General genetic structure of Dulan populations

Principal component cnalysis (PCA) plot of present-day populations and ancient East Asians.

the three groups' substructure among modern Tibetan populations reported by Wang et al.[34] Moreover, we found that Dulan had the closest genetic profiles to the modern core-Tibetan populations. Specifically, Dulan did not share a significant genetic affinity with various reference populations when compared to modern core-Tibetan group, i.e., the Z-score of f_4(Mbuti, reference; core-Tibetan, Dulan) ranging from $-2.16<Z$ to < 1.73 (core-Tibetan group represented by Tibetan_Nagqu); modern corridor-Tibetan group shared an excess affinity with SEA groups compared to Dulan, i.e., the Z-score of f_4(Mbuti, SEA; corridor-Tibetan, Dulan) ranging from $-4.276<Z < -8.884$ (SEA groups represented by Ami); and modern northern-Tibetan group shared an excess affinity with West Eurasian steppe (WES) groups, with a Z-score of f_4(Mbuti, WES; northern-Tibetan, Dulan) ranging from $-2.686<Z < -3.331$ (WES groups represented by EBA_Yamnaya_Samara) (Table S2). In conclusion, we observed that the genetic relationship was closest between Dulan and those representative Tibetan-related populations.

It has long been argued origin of the Tibetan population was associated with the spread of Middle/Late Neolithic farming groups and the Sino-Tibetan languages from the upper Yellow River region to the high-altitude plateau.[7,40,41] In order to comprehensively summarize the phylogenetic relationships of Dulan with other high-altitude East Asian and Middle/Late Neolithic upper Yellow River farmers and reconstruct the population history of Dulan, we next performed the graph-based *qpGraph* analysis.[31,42] Previous studies had failed to model the aMMD and modern Tibetan/Sherpa populations using Middle Neolithic Yellow River population (YR_MN) from Xiaowu and Wanggou sites related to Yangshao-culture, mainly due to the lack of ANA-related ancestry (ANA represented by DevilsCave_N).[24] Thus, we used the Upper_YR_LN as the YR-related source for further analysis. All aMMD and Dulan data fitted our base model (an absolute value of <3 as the worst Z-score indicated an acceptable model) by deriving 81%–91% of their

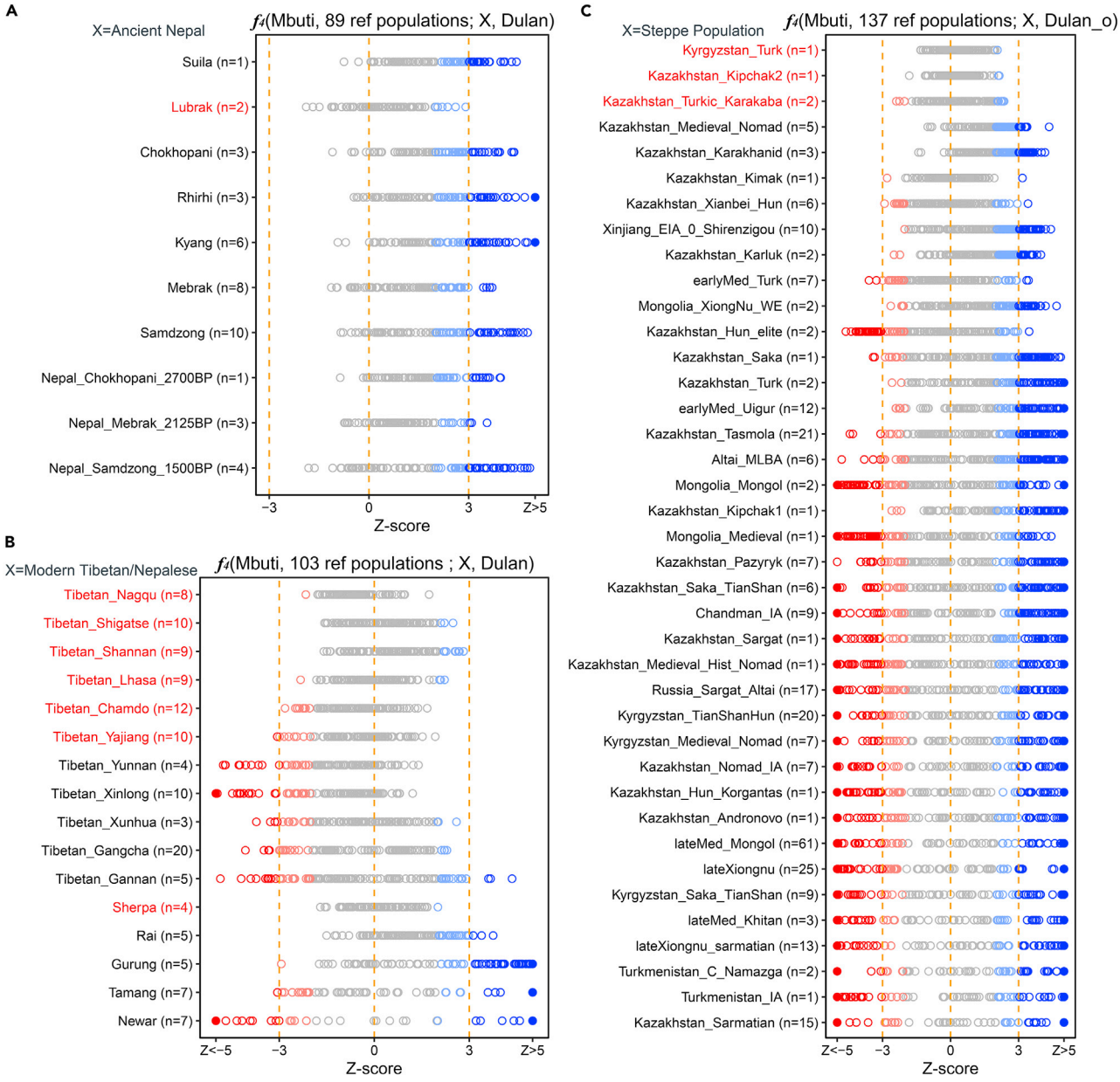

Figure 3. f_4-statistics plots show the genetic affinity of Dulan and Dulan_o

(A) f_4-statistics test in the form of f_4(Mbuti, 89 reference populations; Ancient Nepal, Dulan) indicating the close genetic profiles between Dulan and Lubrak.

(B) f_4-statistics test in the form of f_4(Mbuti, 103 reference populations; Modern Tibetan/Nepalese, Dulan) indicating the close genetic profiles between Dulan and core-Tibetan/Sherpa.

(C) f_4-statistics test in the form of f_4(Mbuti, 137 reference populations; X, Dulan_o) indicating the close genetic profiles between Dulan_o and Kyrgystan_Turk, Kazakhstan_Kipchak2 and Kazakhstan_Turkic_Karakaba, respectively. See more details in Tables S2 and S4. $|Z| \geq 3$ indicated by deep red or blue, $3 > |Z| \geq 2$ indicated in light red or blue.

ancestry from a lineage related to Upper_YR_LN (Figures 4 and S7). As expected, Dulan and Lubrak have the closest proportion of ancestry related to Upper_YR_LN. A complementary analysis leveraged the *f_4-ratio* test[31] and supported the result observed in *qpGraph* (Table S3). Modern-Tibetan populations were modeled on the same graph. Only the modern core-Tibetan populations and modern corridor-Tibetan from Yunnan (Tibetan_Yunnan) fit this model, while modern northern-Tibetan or modern corridor-Tibetan groups provided the absolute value > 3 for the worst Z-score, indicating the possible need for additional gene flow from WES- or SEA-related populations. We then added all modern-Tibetan

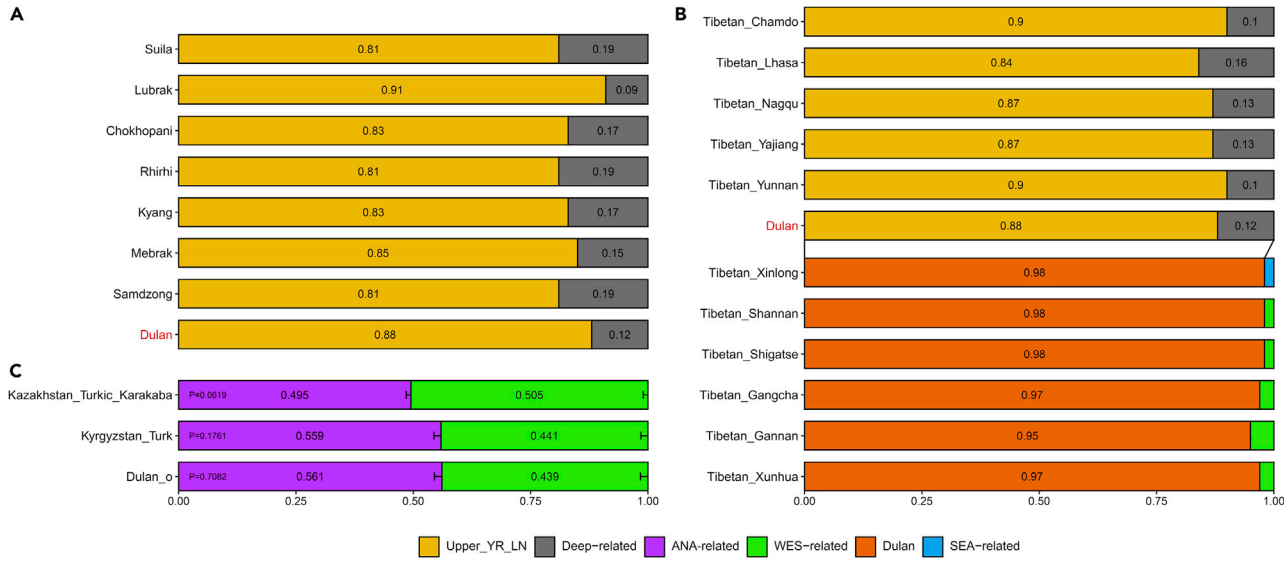

Figure 4. Admixture proportion of target populations

(A) Ancestry proportion estimated for Dulan and aMMD using Upper_YR_LN and an unsampled ancestry via *qpGraph*.

(B) Ancestry proportion estimated for Dulan and modern Tibetans via *qpGraph*.

(C) Ancestry proportion estimated for Dulan_o and relatively close populations via *qpAdm*. Error bars show one standard deviation. See more details in Table S3.

groups to the base model of Dulan. We confirmed that these individuals had received additional gene flow from SEA- or WES- related lineage, in which case all modern-Tibetan groups except one northern-Tibetan from Gannan (Tibetan_Gannan) could provide an acceptable model (Figures S7–S9). Interestingly, modern core-Tibetan populations from Shannan (Tibetan_Shannan) and Shigatse (Tibetan_Shigatse) could provide preferable models when receiving additional gene flow (1%–2%) from WES-related lineage, indicating there might exist the gene flow from WES-related lineage to the modern core-Tibetan populations on central TP, although the relationship was not statistically significant.

EPAS1 is suggested to be the critical factor in the successful settlement of Tibetans in a hypoxic environment.[8,10] The unique Tibetan *EPAS1* haplotype, absent in lowland populations, may have been through introgression from a Denisovan-like population at some point in the distant past.[13,43] We explored the highly differentiated 5-SNP motif of *EPAS1* haplotype (AGGAA, rs115321619, rs73926263, rs73926264, rs73926265, and rs55981512) in the Dulan samples (Table S3). Although coverages across these regions were shallow, we observed 4 and 8 counts for the ancestral and derived SNPs, respectively, for the 5-SNP motif (4/8), compared to YR (32/0 for Upper_YR_LN and 24/0 for Upper_YR_IA) and aMMD (17/1 for Suila, 5/4 for Lubrak, 19/1 for Chokhopani, 38/35 for Rhirhi, 122/182 for Kyang, 131/50 for Mebrak, and 94/84 for Samdzong). Together with the *f*-statistics, these results supported the hypothesis of a core-Tibetan origin of the Tubo-related Dulan population and confirmed a wide distribution of derived *EPAS1* alleles on the TP.

Dulan outlier suggests a possible link between Dulan and West Eurasian steppe populations in the Tubo Empire period

To explore the origin of the Dulan outlier (Dulan_o), we performed the f_4-statistics in the form of f_4(Mbuti, 137 reference populations; X, Dulan_o), where 39 previously reported Eurasian Steppe populations were chosen as X,[15,34–38] and 137 populations from various places were selected as a reference population (Figure 3C and Table S4). Among all the steppe populations, we found the lowest Z-score among three Turk-related populations, with the Z-score of f_4(Mbuti, 137 reference populations; X, Dulan_o) ranging from $-1.32<Z<2.07$, $-1.82<Z<2.15$, and $-2.39<Z<2.36$ when using Kyrgyzstan_Turk (489 CE), Kazakhstan_Kipchak2 (1110 CE), and Kazakhstan_Turkic_Karakaba (7-8th) as X, respectively.[35,36] We next performed the pairwise-*qpWave* analysis (Table S3). The result of pairwise-*qpWave*, however, could not nullify the argument for homogeneity between Dulan_o and any of these three steppe populations (p-value = 0.37, 0.62, and 0.16, respectively). Next, we conducted a *qpAdm* analysis to directly compare the admixture proportion of these four

populations, using four potential sources associated with ANE (represented by Russia_AfontovaGora3), ANA (represented by DevilsCave_N), WES (represented by Russia_MLBA_Sintashta), and Bactria Margiana Archaeological Complex (BMAC, represented by Uzbekistan_BA_Bustan) (Figure 4C and Table S3). We found that Kyrgyzstan_Turk exhibited an almost identical ancestry proportion as Dulan_o. Kazakhstan_Turkic_Karakaba showed heightened WES-related ancestry and reduced ANA-related ancestry when compared with Dulan_o or Kyrgyzstan_Turk, while Kazakhstan_Kipchak2 failed to model with these four potential sources. The assignment of the Y-chromosome haplogroup to R1a1a1b2a-F3568 provided additional support for the origin of Dulan_o from the West Eurasian steppe. In summary, further analyses universally failed to distinguish the Dulan_o and Kyrgyzstan_Turk at the current level resolution. Together with the evidence from the Y-chromosome haplogroup assignment, we therefore suspect some relation between Dulan_o and contemporary Central Asian populations.

DISCUSSION

China's histories tell us how the modern Ganqing region (the primary distribution area of present Amdo Tibetans) was controlled by the Tuyuhun from 313–663 AD before its conquest by the Tubo armies.[22] Subsequent conflict forced the Tubo to migrate a large population into the Ganqing region from the late 7th century onward in order to strengthen area administration and control. The Tubo and Tang empires vied for control of the Ganqing region, affecting the trade network along this eastern stretch of the Silk Road. The dating of individuals unearthed from the Dulan site coincided with the key turning point following the Tubo defeat of the Tuyuhun and exerting control over the Ganqing region. Four burial styles were discovered at Dulan, with the stone chamber tomb (n = 19) the most frequent. This tomb type, which usually has a trapezoidal floor plan, was found frequently on the TP during the Tubo period and perceived as the typical Tubo-style tomb.[44] Burial M17 (supplemental information), for example, the largest stone chamber tomb at Dulan, comprises a mound, burial pit, and burial chamber resembling an adjacent Tubo tomb (No. 99DRNM2) excavated in 1999.[45] Three wooden outer coffin tombs were also found at Dulan. In burial M16, mummified human remains represent a widespread Tubo form of burial. Some unearthed objects carry ink markings in Tibetan, such as oracle bones from M23 and wooden cube-blocks from M16, showing direct evidence of Tubo's influence. A single brick chamber tomb mirrors the influence of a Han culture originating in the Central Plains region.[46] Dulan also contains two earthen pit tombs with a sacrificial horse in the same burial—a burial type found mainly in Turk-related groups across the Altai and Central Asia region, such as early Turk[47] and here turning up unexpectedly in the Ganqing region. Burial M20 consists of a circular stone mound and an earthen burial chamber in this western tradition. Scattered horse bones were also discovered in this burial.

Aside from the earthen pit tomb, the nine individuals in the other three grave types belonged genetically to one homogenous genetic group that was indistinguishable from modern core-Tibetan populations. A parallel study of Yu et al.[26] reported a genetic continuity between ancient Dulan people with ancient Xianbei tribes in Northeast Asia, which we suspected was an overinterpreted signal due to their shallow sequencing data. Our analysis first observed the close relationship between the Dulan people and upper Yellow River farming populations, which confirmed the northern East Asian origin of TP highlanders.[24,34,48] The *qpGraph* modeled the Dulan population as deriving 90% of ancestry from upper Yellow River farmers and the remainder from a deeper unsampled lineage, supporting the multi-wave colonization hypothesis.[18,19] Derived *EPAS1* alleles were commonly found in Dulan and aMMD populations, but unobserved in YR-related populations, suggesting those derived alleles were most likely from a deeper unsampled lineage rather than Yellow River farmers. By comparing the genetic profile of Dulan with aMMD through symmetrical f_4-statistics, we observed a similar genetic composition between Dulan and Lubrak,[24] showing the wide distribution of the Tibetan ancestry on the TP.

Secondly, we investigated the influence of Dulan-related Tubo groups on the formation of modern Tibetans. We observed the close relationship between Dulan and modern core-Tibetan group through the symmetrical f_4-statistics and *qpGraph* modeling. We also observed the genetic flow between WES and SEA groups to the modern northern-Tibetan and modern corridor-Tibetan groups, respectively. Specifically, all the modern core-Tibetan populations and Dulan could be modeled in a two-way admixture by deriving 84%–89% from upper Yellow River farming populations (Upper_YR_LN) and the remainder from an unsampled deep lineage, while modern northern-Tibetan populations could be modeled as deriving 95%–97% from Dulan and the rest from a WES-related ancestry, and modern corridor-Tibetan populations could be modeled as deriving 98%–100% from Dulan and the rest from a SEA-related ancestry. These results indicated a profound influence of Tubo people on modern Tibetans and the genetic continuity of TP highlanders.[16,19]

Consistent with the style of the earthen pit tomb, its occupant, the genetic outlier, was also presumed to be associated with Central Asian steppe populations, particularly with Turk-related populations. We identify the appearance of Central Asian nomads on the Tubo period Tibetan Plateau, implying possible population movements from the Central Asia to the northeast edge of TP under Tubo influence. The assertion is lent additional support by the historical records. Tubo empire formed strategic alliances with Turkic peoples between 7th and 8th centuries CE. In the year 734, the Tubo princess Zhuomagi was married to Sulu, Khan of Turgesh (an ancient Turkic ethnic group). Frequent contacts occurred between the Tubo and Central Asian ethnic groups, among them Turks and Sogdians.[49] The occupation of Ganqing region by the Tubo empire would not only sever the connection between the Western regions and the Tang Dynasty but also won the Tubo control over the West-East trade network. Aside from jewelry and local products, the Tubo people sold a large number of goods to Central Asia. These included musk, gold, silver, medicine, salt, and horses. Traders from traveling in the opposite direction—nomads of the Central Asian Steppe—carried with them weapons, textiles, and knowledge of Christianity and Islam.[50]

This picture of population dynamics on the TP has largely been obscured by sparse ancient DNA sampling. Our newly generated data shed more light on the constitution of the Tubo population and provide direct evidence of communications between Tibetan highlanders and the Central Asian steppe. Future expansion in the sample size and excavations will be sure to provide further insights into TP population history. The Dulan site has the possibility of bringing us further back in TP historical type, with Tuyuhun period burials located at nearby Xuewei Tomb No.1 (2018DRXM1), presumed to be the final resting place of the Mohetuhun Khan, the King of Tuyuhun.[51] Notably, during the late Bronze Age, the Dulan district was occupied by ancient populations belonging to the Nuomuhong culture.[52] Then, since the late Western Jin Dynasty, this area was once the heartland of Tuyuhun,[53] and subsequently annexed by Tubo. Thus, future studies of ancient genomes across the northeast edge of TP, especially the local Nuomuhong-related and Tuyuhun-related samples, will undoubtedly help our understanding of the population history of the northern TP.

Limitations of the study

The Dulan district has large numbers of tombs with different burial types and tomb sizes. More sampling in Dulan site is needed to comprehensively clarify the genetic profiles of Dulan population. The lack of ancient samples of contemporaneous core-Tibetan groups disenables the direct compare of genetic profiles of Dulan population with the ancient individuals of the Tubo Empire. Further sampling in core-Tibetan regions will be sure to provide further insights into TP population history.

STAR★METHODS

Detailed methods are provided in the online version of this paper and include the following:

- KEY RESOURCES TABLE
- RESOURCE AVAILABILITY
  - Lead contact
  - Materials availability
  - Data and code availability
- EXPERIMENTAL MODEL AND SUBJECT DETAILS
  - Archaeological and anthropological information
  - Radiocarbon dating of sample materials
- METHOD DETAILS
  - Ancient DNA extraction and library preparation
- QUANTIFICATION AND STATISTICAL ANALYSIS
  - Sequence data processing
  - Authentication of ancient DNA
  - Genetic sexing and uniparental haplogroup assignment
  - Kinship detection
  - Data merging
  - Principal components analysis
  - ADMIXTURE analysis
  - *f*-statistics
  - *qpWave* analysis
  - Admixture modelling

SUPPLEMENTAL INFORMATION

Supplemental information can be found online at https://doi.org/10.1016/j.isci.2022.105636.

ACKNOWLEDGMENTS

The work was funded by the National Natural Science Foundation of China (31801040, 32070576, and 32270667), Priority Research Program of the Chinese Academy of Sciences: Pan-Third Pole Environment Study for a Green Silk Road (Pan-TPE) (Grant No. XDA2004010101), the "Double First Class University Plan" key construction project of Xiamen University (0310/X2106027), Nanqiang Outstanding Young Talents Program of Xiamen University (X2123302), the National Social Science Fund of China (19VJX074 and 21CKG022), the Science and Technology Commission of Shanghai Municipality (18490750300), the National Key Research and Development Program (2020YFE0201600), Shanghai Municipal Science and Technology Major Project (2017SHZDZX01), the Major Project of National Social Science Foundation of China granted to C.C.W. (21&ZD285) and S.W. (20&ZD212), Major Special Project of Philosophy and Social Sciences Research of the Ministry of Education (2022JZDZ023), and European Research Council (ERC) grant (ERC-2019-ADG-883700-TRAM).

AUTHOR CONTRIBUTIONS

S.W. and C.C.W. conducted the project and conceived the idea. P.D., J.L., J.Z., X.H., H.M., J.X., X.R., Y.D., Y.X., X.C., and G.D. collected the samples and carried out the experiments. K.Z., B.Z., and C.C.W. analyzed the data. K.Z., P.D., E.A., C.C.W., and S.W. wrote the paper. P.D. and K.Z. wrote and edited the supplementary text. All the authors revised the paper.

DECLARATION OF INTERESTS

The authors declare no competing interests.

Received: September 14, 2022
Revised: October 15, 2022
Accepted: November 17, 2022
Published: December 22, 2022

REFERENCES

1. Zhang, J.F., and Dennell, R. (2018). The last of Asia conquered by Homo sapiens Excavation reveals the earliest human colonization of the Tibetan Plateau. Science *362*, 992–993. https://doi.org/10.1126/science.aav6863.

2. Zhang, D., Xia, H., Chen, F., Li, B., Slon, V., Cheng, T., Yang, R., Jacobs, Z., Dai, Q., Massilani, D., et al. (2020). Denisovan DNA in late pleistocene sediments from Baishiya Karst Cave on the Tibetan plateau. Science *370*, 584–587. https://doi.org/10.1126/science.abb6320.

3. Chen, F., Welker, F., Shen, C.C., Bailey, S.E., Bergmann, I., Davis, S., Xia, H., Wang, H., Fischer, R., Freidline, S.E., et al. (2019). A late Middle pleistocene denisovan mandible from the Tibetan plateau. Nature *569*, 409–412. https://doi.org/10.1038/s41586-019-1139-x.

4. Zhang, X.L., Ha, B.B., Wang, S.J., Chen, Z.J., Ge, J.Y., Long, H., He, W., Da, W., Nian, X.M., Yi, M.J., et al. (2018). The earliest human occupation of the high-altitude Tibetan Plateau 40 thousand to 30 thousand years ago. Science *362*, 1049–1051. https://doi.org/10.1126/science.aat8824.

5. Zhang, D.D., and Li, S.H. (2002). Optical dating of Tibetan human hand- and footprints: an implication for the palaeoenvironment of the last glaciation of the Tibetan Plateau. Geophys. Res. Lett. *29*, 16-1–16-3. https://doi.org/10.1029/2001gl013749.

6. Meyer, M.C., Aldenderfer, M.S., Wang, Z., Hoffmann, D.L., Dahl, J.A., Degering, D., Haas, W.R., and Schlütz, F. (2017). Permanent human occupation of the central Tibetan Plateau in the early Holocene. Science *355*, 64–67. https://doi.org/10.1126/science.aag0357.

7. Chen, F.H., Dong, G.H., Zhang, D.J., Liu, X.Y., Jia, X., An, C.B., Ma, M.M., Xie, Y.W., Barton, L., Ren, X.Y., et al. (2015). Agriculture facilitated permanent human occupation of the Tibetan Plateau after 3600 B.P. Science *347*, 248–250. https://doi.org/10.1126/science.1259172.

8. Gnecchi-Ruscone, G.A., Abondio, P., De Fanti, S., Sarno, S., Sherpa, M.G., Sherpa, P.T., Marinelli, G., Natali, L., Di Marcello, M., Peluzzi, D., et al. (2018). Evidence of polygenic adaptation to high altitude from Tibetan and Sherpa genomes. Genome Biol. Evol. *10*, 2919–2930. https://doi.org/10.1093/gbe/evy233.

9. Qi, X., Cui, C., Peng, Y., Zhang, X., Yang, Z., Zhong, H., Zhang, H., Xiang, K., Cao, X., Wang, Y., et al. (2013). Genetic evidence of paleolithic colonization and neolithic expansion of modern humans on the Tibetan plateau. Mol. Biol. Evol. *30*, 1761–1778. https://doi.org/10.1093/molbev/mst093.

10. Beall, C.M., Cavalleri, G.L., Deng, L., Elston, R.C., Gao, Y., Knight, J., Li, C., Li, J.C., Liang, Y., McCormack, M., et al. (2010). Natural selection on EPAS1 (HIF2alpha) associated with low hemoglobin concentration in Tibetan highlanders. Proc. Natl. Acad. Sci. USA *107*, 11459–11464. https://doi.org/10.1073/pnas.1002443107.

11. Simonson, T.S., Yang, Y., Huff, C.D., Yun, H., Qin, G., Witherspoon, D.J., Bai, Z., Lorenzo, F.R., Xing, J., Jorde, L.B., et al. (2010). Genetic evidence for high-altitude adaptation in Tibet. Science *329*, 72–75. https://doi.org/10.1126/science.1189406.

12. Yi, X., Liang, Y., Huerta-Sanchez, E., Jin, X., Cuo, Z.X.P., Pool, J.E., Xu, X., Jiang, H., Vinckenbosch, N., Korneliussen, T.S., et al. (2010). Sequencing of 50 human exomes reveals adaptation to high altitude. Science *329*, 75–78. https://doi.org/10.1126/science.1190371.

13. Huerta-Sánchez, E., Jin, X., Asan, Bianba, Z., Bianba, Z., Peter, B.M., Vinckenbosch, N., Liang, Y., Yi, X., He, M., Somel, M., et al. (2014). Altitude adaptation in Tibetans

caused by introgression of Denisovan-like DNA. Nature *512*, 194–197. https://doi.org/10.1038/nature13408.

14. Xiang, K., Ouzhuluobu, Peng, Y., Peng, Y., Yang, Z., Zhang, X., Cui, C., Zhang, H., Li, M., Zhang, Y., Bianba, et al.. (2013). Identification of a Tibetan-specific mutation in the hypoxic gene EGLN1 and its contribution to high-altitude adaptation. Mol. Biol. Evol. *30*, 1889–1898. https://doi.org/10.1093/molbev/mst090.

15. Ning, C., Li, T., Wang, K., Zhang, F., Li, T., Wu, X., Gao, S., Zhang, Q., Zhang, H., Hudson, M.J., et al. (2020). Ancient genomes from northern China suggest links between subsistence changes and human migration. Nat. Commun. *11*, 2700. https://doi.org/10.1038/s41467-020-16557-2.

16. Zhao, M., Kong, Q.P., Wang, H.W., Peng, M.S., Xie, X.D., Wang, W.Z., Jiayang, Duan, J.G., Duan, J.G., Cai, M.C., Zhao, S.N., et al. (2009). Mitochondrial genome evidence reveals successful Late Paleolithic settlement on the Tibetan Plateau. Proc. Natl. Acad. Sci. USA *106*, 21230–21235. https://doi.org/10.1073/pnas.0907844106.

17. Qin, Z., Yang, Y., Kang, L., Yan, S., Cho, K., Cai, X., Lu, Y., Zheng, H., Zhu, D., Fei, D., et al. (2010). A mitochondrial revelation of early human migrations to the Tibetan Plateau before and after the last glacial maximum. Am. J. Phys. Anthropol. *143*, 555–569. https://doi.org/10.1002/ajpa.21350.

18. Li, Y.C., Tian, J.Y., and Kong, Q.P. (2015). A dual origin of Tibetans: evidence from mitochondrial genomes. J. Hum. Genet. *60*, 403–404. https://doi.org/10.1038/jhg.2015.40.

19. Lu, D., Lou, H., Yuan, K., Wang, X., Wang, Y., Zhang, C., Lu, Y., Yang, X., Deng, L., Zhou, Y., et al. (2016). Ancestral origins and genetic history of Tibetan highlanders. Am. J. Hum. Genet. *99*, 580–594. https://doi.org/10.1016/j.ajhg.2016.07.002.

20. Cai, R. (2007). The History of Tubo (In Chinese) (Gansu people's publishing house).

21. Wang, S.C. (2012). The Phonetic Research of Amdo Tibetan Dialect (In Chinese) (Zhongxi book company).

22. Zhou, W.Z. (2006). The History of Tuyuhun (In Chinese) (Guangxi Normal University Press).

23. Jeong, C., Ozga, A.T., Witonsky, D.B., Malmström, H., Edlund, H., Hofman, C.A., Hagan, R.W., Jakobsson, M., Lewis, C.M., Aldenderfer, M.S., et al. (2016). Long-term genetic stability and a high-altitude East Asian origin for the peoples of the high valleys of the Himalayan arc. Proc. Natl. Acad. Sci. USA *113*, 7485–7490. https://doi.org/10.1073/pnas.1520844113.

24. Liu, C.C., Witonsky, D., Gosling, A., Lee, J.H., Ringbauer, H., Hagan, R., Patel, N., Stahl, R., Novembre, J., Aldenderfer, M., et al. (2022). Ancient genomes from the Himalayas illuminate the genetic history of Tibetans and their Tibeto-Burman speaking neighbors. Nat. Commun. *13*, 1203. https://doi.org/10.1038/s41467-022-28827-2.

25. Yang, X.Y., Rakha, A., Chen, W., Hou, J., Qi, X.B., Shen, Q.K., Dai, S.S., Sulaiman, X., Abdulloevich, N.T., Afanasevna, M.E., et al. (2021). Tracing the genetic legacy of the Tibetan empire in the Balti. Mol. Biol. Evol. *38*, 1529–1536. https://doi.org/10.1093/molbev/msaa313.

26. Yu, X.E., Sun, C., Zou, Y.T., Li, J.Y., Ren, X., and Li, H. (2022). Ancient DNA from Tubo Kingdom-related tombs in northeastern Tibetan Plateau revealed their genetic affinity to both Tibeto-Burman and Altaic populations. Mol. Genet. Genom. *297*, 1755–1765. https://doi.org/10.1007/s00438-022-01955-6.

27. Jónsson, H., Ginolhac, A., Schubert, M., Johnson, P.L.F., and Orlando, L. (2013). mapDamage2.0: fast approximate Bayesian estimates of ancient DNA damage parameters. Bioinformatics *29*, 1682–1684. https://doi.org/10.1093/bioinformatics/btt193.

28. Lipatov, M., Sanjeev, K., Patro, R., and Veeramah, K.R. (2015). Maximum likelihood estimation of biological relatedness from low coverage sequencing data. Preprint at bioRxiv. https://doi.org/10.1101/023374.

29. Renaud, G., Slon, V., Duggan, A.T., and Kelso, J. (2015). Schmutzi: estimation of contamination and endogenous mitochondrial consensus calling for ancient DNA. Genome Biol. *16*, 224. https://doi.org/10.1186/s13059-015-0776-0.

30. Korneliussen, T.S., Albrechtsen, A., and Nielsen, R. (2014). ANGSD: analysis of next generation sequencing data. BMC Bioinf. *15*, 356. https://doi.org/10.1186/s12859-014-0356-4.

31. Patterson, N., Moorjani, P., Luo, Y., Mallick, S., Rohland, N., Zhan, Y., Genschoreck, T., Webster, T., and Reich, D. (2012). Ancient admixture in human history. Genetics *192*, 1065–1093. https://doi.org/10.1534/genetics.112.145037.

32. Yang, M.A., Fan, X., Sun, B., Chen, C., Lang, J., Ko, Y.C., Tsang, C.H., Chiu, H., Wang, T., Bao, Q., et al. (2020). Ancient DNA indicates human population shifts and admixture in northern and southern China. Science *369*, 282–288. https://doi.org/10.1126/science.aba0909.

33. McColl, H., Racimo, F., Vinner, L., Demeter, F., Gakuhari, T., Moreno-Mayar, J.V., van Driem, G., Gram Wilken, U., Seguin-Orlando, A., de la Fuente Castro, C., et al. (2018). The prehistoric peopling of Southeast Asia. Science *361*, 88–92. https://doi.org/10.1126/science.aat3628.

34. Wang, C.-C., Yeh, H.-Y., Popov, A.N., Zhang, H.-Q., Matsumura, H., Sirak, K., Cheronet, O., Kovalev, A., Rohland, N., Kim, A.M., et al. (2021). Genomic insights into the formation of human populations in East Asia. Nature *591*, 413–419. https://doi.org/10.1038/s41586-021-03336-2.

35. Damgaard, P.d.B., Marchi, N., Rasmussen, S., Peyrot, M., Renaud, G., Korneliussen, T., Moreno-Mayar, J.V., Pedersen, M.W., Goldberg, A., Usmanova, E., et al. (2018). 137 ancient human genomes from across the Eurasian steppes. Nature *557*, 369–374. https://doi.org/10.1038/s41586-018-0094-2.

36. Gnecchi-Ruscone, G.A., Khussainova, E., Kahbatkyzy, N., Musralina, L., Spyrou, M.A., Bianco, R.A., Radzeviciute, R., Martins, N.F.G., Freund, C., Iksan, O., et al. (2021). Ancient genomic time transect from the Central Asian Steppe unravels the history of the Scythians. Sci. Adv. *7*, eabe4414. https://doi.org/10.1126/sciadv.abe4414.

37. Jeong, C., Wang, K., Wilkin, S., Taylor, W.T.T., Miller, B.K., Bemmann, J.H., Stahl, R., Chiovelli, C., Knolle, F., Ulziibayar, S., et al. (2020). A dynamic 6, 000-year genetic history of eurasia's eastern steppe. Cell *183*, 890–904.e29. https://doi.org/10.1016/j.cell.2020.10.015.

38. Ning, C., Wang, C.C., Gao, S., Yang, Y., Zhang, X., Wu, X., Zhang, F., Nie, Z., Tang, Y., Robbeets, M., et al. (2019). Ancient genomes reveal yamnaya-related ancestry and a potential source of indo-European speakers in iron Age tianshan. Curr. Biol. *29*, 2526–2532.e4. https://doi.org/10.1016/j.cub.2019.06.044.

39. Patterson, N., Price, A.L., and Reich, D. (2006). Population structure and eigenanalysis. PLoS Genet. *2*, e190. https://doi.org/10.1371/journal.pgen.0020190.

40. Sagart, L., Jacques, G., Lai, Y., Ryder, R.J., Thouzeau, V., Greenhill, S.J., and List, J.M. (2019). Dated language phylogenies shed light on the ancestry of Sino-Tibetan. Proc. Natl. Acad. Sci. USA *116*, 10317–10322. https://doi.org/10.1073/pnas.1817972116.

41. Zhang, M., Yan, S., Pan, W., and Jin, L. (2019). Phylogenetic evidence for Sino-Tibetan origin in northern China in the late neolithic. Nature *569*, 112–115. https://doi.org/10.1038/s41586-019-1153-z.

42. Reich, D., Thangaraj, K., Patterson, N., Price, A.L., and Singh, L. (2009). Reconstructing Indian population history. Nature *461*, 489–494. https://doi.org/10.1038/nature08365.

43. Browning, S.R., Browning, B.L., Zhou, Y., Tucci, S., and Akey, J.M. (2018). Analysis of human sequence data reveals two pulses of archaic denisovan admixture. Cell *173*, 53–61.e9. https://doi.org/10.1016/j.cell.2018.02.031.

44. Hu, X.J., Chen, H.Q., Zhang, J.L., Liang, G.J., Shi, J., and Jin, P. (2018). The excavation of Wayan reservoir site of Dulan county, Qinghai in 2014 (in Chinese). Archaeol. Cult. Relics, 30–50.

45. School of Archaeology and Museology of Peking University & Qinghai Provincial Institute of Archaeology (2005). Dulan Tubo tomb No.2. In Tibetan tombs at Dulan Qinghai (in Chinese), J.W. Luo, ed. (Beijing: Science Press), pp. 32–42.

46. Ramsey, C.B., and Lee, S. (2013). Recent and planned developments of the program oxcal. Radiocarbon *55*, 720–730.

47. Konstantinov, N., Soenov, V., Trifanova, S., and Svyatko, S. (2018). History and culture of the early Türkic period: a review of archaeological monuments in the Russian Altai from the 4th–6th century AD. Archaeol. Res. Asia *16*, 103–115. https://doi.org/10.1016/j.ara.2018.06.002.

48. He, G., Wang, M., Zou, X., Chen, P., Wang, Z., Liu, Y., Yao, H., Wei, L.H., Tang, R., Wang, C.C., and Yeh, H.Y. (2021). Peopling history of the Tibetan plateau and multiple waves of admixture of Tibetans inferred from both ancient and modern genome-wide data. Front. Genet. *12*, 725243. https://doi.org/10.3389/fgene.2021.725243.

49. Stein, R.A. (1972). Historical survey. In Tibetan Civilization (Stanford University Press), p. 64.

50. Ferrand, G. (1913). Travel Journeys and Arabic, Persian and Turkish Geographical Texts on the Far East from the 8th through 18th centuries (in French).

51. Han, J.H., Bai, L.W., Zhen, Q., Shi, J., and Zhang, G.G. (2021). The excavation of Xuewei tomb No.1 of Reshui tomb cluster from dulan county, Qinghai in 2018. Archaeology *647*, 45–70.

52. Wu, R.X. (1963). The excavation of Talitaliha site of Dulan county, Qinghai (in Chinese). Acta Archaeol. Sin. *01*, 17–44+148.

53. Li, W.X. (2007). A Study on Tuyuhun (Lanzhou University).

54. Schubert, M., Lindgreen, S., and Orlando, L. (2016). AdapterRemoval v2: rapid adapter trimming, identification, and read merging. BMC Res. Notes *9*, 88. https://doi.org/10.1186/s13104-016-1900-2.

55. Li, H., and Durbin, R. (2009). Fast and accurate short read alignment with Burrows-Wheeler transform. Bioinformatics *25*, 1754–1760. https://doi.org/10.1093/bioinformatics/btp324.

56. Peltzer, A., Jäger, G., Herbig, A., Seitz, A., Kniep, C., Krause, J., and Nieselt, K. (2016). EAGER: efficient ancient genome reconstruction. Genome Biol. *17*, 60. https://doi.org/10.1186/s13059-016-0918-z.

57. Weissensteiner, H., Pacher, D., Kloss-Brandstätter, A., Forer, L., Specht, G., Bandelt, H.J., Kronenberg, F., Salas, A., and Schönherr, S. (2016). HaploGrep 2: mitochondrial haplogroup classification in the era of high-throughput sequencing. Nucleic Acids Res. *44*, W58–W63. https://doi.org/10.1093/nar/gkw233.

58. Ralf, A., Montiel González, D., Zhong, K., and Kayser, M. (2018). Yleaf: software for human Y-chromosomal haplogroup inference from next-generation sequencing data. Mol. Biol. Evol. *35*, 1291–1294. https://doi.org/10.1093/molbev/msy032.

59. Thorvaldsdóttir, H., Robinson, J.T., and Mesirov, J.P. (2013). Integrative Genomics Viewer (IGV): high-performance genomics data visualization and exploration. Brief. Bioinform. *14*, 178–192. https://doi.org/10.1093/bib/bbs017.

60. Alexander, D.H., Novembre, J., and Lange, K. (2009). Fast model-based estimation of ancestry in unrelated individuals. Genome Res. *19*, 1655–1664. https://doi.org/10.1101/gr.094052.109.

61. Huo, W. (1995). Grave System in Ancient Tibet (In Chinese) (Sichuan Renmin Press).

62. Sun, J. (2015). Study on the Factors of Burial Culture in Haixi of Qinghai Area from Five to Eight Century (Northwest Normal University).

63. Chu, J.J. (1989). The study of Tubo Bon's funeral ritual procedure interpreted based on Dunhuang documents P.T.1042. In ancient Tibetan language (in Chinese), pp. 15–34.

64. Yu, X.H., and Wang, W. (2021). The influence of central Plains culture on the formation of Tubo tomb system (in Chinese). J. Xizang Minzu Univer. (Philosophy and Social Sciences Edition) *42*, 92–98. 156.

65. Reimer, P.J., Austin, W.E.N., Bard, E., Bayliss, A., Blackwell, P.G., Bronk Ramsey, C., Butzin, M., Cheng, H., Edwards, R.L., Friedrich, M., et al. (2020). The Intcal20 northern hemisphere radiocarbon Age calibration curve (0-55 cal kbp). Radiocarbon *62*, 725–757.

66. Zhu, K., Du, P., Xiong, J., Ren, X., Sun, C., Tao, Y., Ding, Y., Xu, Y., Meng, H., Wang, C.C., and Wen, S.Q. (2021). Comparative performance of the MGISEQ-2000 and Illumina X-ten sequencing platforms for paleogenomics. Front. Genet. *12*, 745508. https://doi.org/10.3389/fgene.2021.745508.

67. Knapp, M., Clarke, A.C., Horsburgh, K.A., and Matisoo-Smith, E.A. (2012). Setting the stage - building and working in an ancient DNA laboratory. Ann. Anat. *194*, 3–6. https://doi.org/10.1016/j.aanat.2011.03.008.

68. Meyer, M., and Kircher, M. (2010). Illumina sequencing library preparation for highly multiplexed target capture and sequencing. Cold Spring Harb. Protoc. *2010*. pdb.prot5448. https://doi.org/10.1101/pdb.prot5448.

69. Gamba, C., Jones, E.R., Teasdale, M.D., McLaughlin, R.L., Gonzalez-Fortes, G., Mattiangeli, V., Domboróczki, L., Kővári, I., Pap, I., Anders, A., et al. (2014). Genome flux and stasis in a five millennium transect of European prehistory. Nat. Commun. *5*, 5257. https://doi.org/10.1038/ncomms6257.

70. Allentoft, M.E., Sikora, M., Sjögren, K.G., Rasmussen, S., Rasmussen, M., Stenderup, J., Damgaard, P.B., Schroeder, H., Ahlström, T., Vinner, L., et al. (2015). Population genomics of bronze Age Eurasia. Nature *522*, 167–172. https://doi.org/10.1038/nature14507.

71. Sun, X.F., Wen, S.Q., Lu, C.Q., Zhou, B.Y., Curnoe, D., Lu, H.Y., Li, H.C., Wang, W., Cheng, H., Yi, S.W., et al. (2021). Ancient DNA and multimethod dating confirm the late arrival of anatomically modern humans in southern China. Proc. Natl. Acad. Sci. USA *118*. e2019158118. https://doi.org/10.1073/pnas.2019158118.

72. Mittnik, A., Wang, C.C., Svoboda, J., and Krause, J. (2016). A molecular approach to the sexing of the triple burial at the upper paleolithic site of dolni vestonice. PLoS One *11*, e0163019. https://doi.org/10.1371/journal.pone.0163019.

73. Skoglund, P., Storå, J., Götherström, A., and Jakobsson, M. (2013). Accurate sex identification of ancient human remains using DNA shotgun sequencing. J. Archaeol. Sci. *40*, 4477–4482. https://doi.org/10.1016/j.jas.2013.07.004.

74. Chang, C.C., Chow, C.C., Tellier, L.C., Vattikuti, S., Purcell, S.M., and Lee, J.J. (2015). Second-generation PLINK: rising to the challenge of larger and richer datasets. GigaScience *4*, 7. https://doi.org/10.1186/s13742-015-0047-8.

75. Peter, B.M. (2016). Admixture, population structure, and F-statistics. Genetics *202*, 1485–1501. https://doi.org/10.1534/genetics.115.183913.

76. Lawson, D.J., van Dorp, L., and Falush, D. (2018). A tutorial on how not to over-interpret STRUCTURE and ADMIXTURE bar plots. Nat. Commun. *9*, 3258. https://doi.org/10.1038/s41467-018-05257-7.

77. Haak, W., Lazaridis, I., Patterson, N., Rohland, N., Mallick, S., Llamas, B., Brandt, G., Nordenfelt, S., Harney, E., Stewardson, K., et al. (2015). Massive migration from the steppe was a source for Indo-European languages in Europe. Nature *522*, 207–211. https://doi.org/10.1038/nature14317.

78. Harney, E., Patterson, N., Reich, D., and Wakeley, J. (2021). Assessing the performance of qpAdm: a statistical tool for studying population admixture. Genetics *217*. https://doi.org/10.1093/genetics/iyaa045.

79. Wang, T., Wang, W., Xie, G., Li, Z., Fan, X., Yang, Q., Wu, X., Cao, P., Liu, Y., Yang, R., et al. (2021). Human population history at the crossroads of East and Southeast Asia since 11, 000 years ago. Cell *184*, 3829–3841.e21. https://doi.org/10.1016/j.cell.2021.05.018.

STAR★METHODS

KEY RESOURCES TABLE

REAGENT or RESOURCE	SOURCE	IDENTIFIER
Biological samples		
Ancient human remains	This paper	BB2004
Ancient human remains	This paper	BB2005
Ancient human remains	This paper	BB2006
Ancient human remains	This paper	BB2007
Ancient human remains	This paper	BB2008
Ancient human remains	This paper	BB2009
Ancient human remains	This paper	BB2010
Ancient human remains	This paper	BB2011
Ancient human remains	This paper	BB2012
Ancient human remains	This paper	BB2013
Chemicals, peptides, and recombinant proteins		
EDTA (0.5M, pH 8.0)	Sangon Biotech	B540625-0500
Proteinase K	Merck	539480
Extraction bead	Enlighten Biotech	LD101
Guanidine hydrochloride	Sigma Aldrich	50933
Isopropanol	Sigma Aldrich	67-63-0
Sodium acetate	Sigma Aldrich	S2889
Tween-20	Sigma Aldrich	P9416
ATP	Thermo	R0441
dNTP Mix	Thermo	R1121
T4 DNA Ligase	Thermo	EL0011
T4 Polynucleotide Kinase	New England Biolabs	M0236L
T4 DNA Polymerase	New England Biolabs	M0203L
Bst enzyme	New England Biolabs	M0275S
Q5 High-Fidelity DNA Polymerase	New England Biolabs	M0491S
BSA 20mg/mL	New England Biolabs	B9000S
Agencourt AMPure XP beads	Beckman Coulter	A63881
Critical commercial assays		
MGI Easy Universal Library Conversion Kit (App-A)	MGI	1000004155
MGISEQ-2000RS High-throughput (Rapid) Sequencing Kit (App-A, PE100)	MGI	1000005662
Min Elute PCR Purification Kit	QIAGEN	28006
Quick Ligation Kit	New England Biolabs	M2200
Deposited data		
BAM files are available in the BIG Data Center Genome Sequence Archive (http://bigd.big.ac.cn/gsa-human/)	This paper	HRA003047
Software and algorithms		
AdapterRemoval v2.3.1	Schubert et al.[54]	https://github.com/MikkelSchubert/adapterremoval; RRID:SCR_011834
BWA v0.7.17	Li et al.[55]	https://bio-bwa.sourceforge.net/; RRID:SCR_010910

(*Continued on next page*)

Continued

REAGENT or RESOURCE	SOURCE	IDENTIFIER
bamUtil v1.0.14	https://github.com/statgen/bamUtil	https://github.com/statgen/bamUtil
DeDup v0.12.3	Peltzer et al.[56]	https://github.com/apeltzer/DeDup
pileupCaller	https://github.com/stschiff/sequenceTools	https://github.com/stschiff/sequenceTools
mapDamage v2.0	Jonsson et al.[27]	https://ginolhac.github.io/mapDamage/; RRID:SCR_001240
ANGSD v0.931	Korneliussen et al.[30]	http://www.popgen.dk/angsd/index.php/ANGSD; RRID:SCR_021865
Schmutzi v1.5.5.5	Renaud et al.[29]	https://github.com/grenaud/schmutzi
HaploGrep2	Weissensteiner et al.[57]	https://haplogrep.uibk.ac.at/index.html
Yleaf	Ralf et al.[58]	https://github.com/genid/Yleaf
IGV	Thorvaldsdottir et al.[59]	https://igv.org/; RRID:SCR_011793
EIGENSOFT v7.2.1	Patterson et al.[39]	https://github.com/DReichLab/EIG; RRID:SCR_004965
ADMIXTOOLS v7.0.2	Patterson et al.[31]	https://github.com/DReichLab/AdmixTools/; RRID:SCR_018495
ADMIXTURE v1.3.0	Alexander et al.[60]	http://dalexander.github.io/admixture/index.html; RRID:SCR_001263
lcMLkin	Lipatov et al.[28]	https://github.com/COMBINE-lab/maximum-likelihood-relatedness-estimation

RESOURCE AVAILABILITY

Lead contact

Further information and requests for resources and reagents should be directed to and will be fulfilled by the lead contact, S. Wen(wenshaoqing@fudan.edu.cn).

Materials availability

This study did not generate new unique reagents.

Data and code availability

- All data needed to evaluate the conclusions in the paper are present in the paper and/or the supplemental information. Raw FastQ and alignment files (BAM format) are available at the Genome Warehouse in National Genomics Data Center, Beijing Institute of Genomics (China National Center for Bioinformation), Chinese Academy of Sciences, under accession number HRA003047, which is publicly accessible at https://bigd.big.ac.cn/gsa-human/. Haploid genotype data of ancient individuals in this study on the 1240K panel are available in the EIGENSTRAT format from the following link:https://reich.hms.harvard.edu/allen-ancient-dna-resource-aadr-downloadable-genotypes-present-day-and-ancient-dna-data.
- This paper does not report original code.
- Any additional information required to reanalyze the data reported in this paper is available from the lead contact upon request.

EXPERIMENTAL MODEL AND SUBJECT DETAILS

Archaeological and anthropological information

We collected a total of 10 ancient samples from the Dulan site (Tables 1 and S1). Approval for their use was curated by co-authors and obtained with permission from the respective provincial archaeology institutes or universities that managed the samples. The permission and oversight were also provided by the institutional review board at the Ethics Committee for Biological Research at Fudan University.

The Dulan site is located around 2km southeast of Zamari village in Reshui town in Dulan county, Qinghai province.[44] From April to September of 2014, the Qinghai Provincial Institute of Archaeology and Shaanxi Provincial Institute of Archaeology jointly conducted a salvage archaeology project at the site. A total of 25 tombs and 5 sacrificial horse pits were excavated in this joint archaeological campaign. A wealth of grave goods were unearthed despite prior severe looting. Burial features including burial styles, burial customs, sacrificial methods and grave goods indicated typical Tubo style grave traits. The Dulan site can therefore provide key empirical data for studying the history of the Dulan area, territorial shifts within the Tubo Empire and cultural exchanges between the Western Regions, Tang Empire and Tubo Empire.

Since 7th century AD, the ancient Tibetan people began to flourish out in the Yalong River Valley of Shannan region, unify surrounding tribes and then establish the Tubo Empire. By conducting series of military campaigns, the Tubo Empire controlled territory of 4 million km,^{2} spanning parts of East Asia, Central Asia, and South Asia (Figure S10).

Dulan is situated nearby the Wayan reservoir, along the Chahanwusu River (察汗乌苏河). A total of 23 tombs lie on the south bank of the Chahanwusu, and only 2 on the north bank. Dulan could be further classified into four groups based on discernible grave typologies: vertical earthen pit tomb with stone chamber tomb, vertical earthen pit tomb with wooden outer coffin, vertical earthen pit tomb and vertical earthen pit tomb with brick chamber. These burial types and their grave good content are briefly introduced below:

Stone chamber tomb: Dulan's 19 stone chamber tombs can be subdivided into 1 large, 3 medium and 15 small tombs (Figure S11). After removing the residual soil or stone mound, tomb floor plans are mostly trapezoidal, similar to other Tubo tombs on the Tibetan Plateau.[45,61] M17 occupies a core location in the cemetery and is the largest stone chamber tomb (Figures S12 and S13). This burial comprises a mound, burial pit and burial chamber. Though the mound was severely damaged, the stone frame and adobe base could still be found. Examined from above, the stone frame is trapezoidal, measuring 9.9 m from north to south and 8.2–12.5 m from east to west. In general, the burial style and scale resemble the adjacent Tubo tomb (No. 99DRNM2) excavated in 1999.[45] In particular, two burnt phalanxes were found in M4, which may indicate cremation burial. Burial M8 also consists of mound, burial pit and burial chamber (Figure S14). The burial pit is trapezoidal, measuring 2.42–3.82 m from east to west, 3.15 m from north to south. Since the burial pit is short and the stone burial chamber is closely flattened against the inside of the burial pit, the pit height is nearly the same as the chamber height, at 0.85 m. No coffin apparatus was found and only fragmented skeletons were discovered in a looter's shaft. About 2.3 m southeast of M8, M25 is nearly rectangular with an inner wall of stone masonry, measuring 1.17 m from east to west, 0.47–0.97 m from north to south, 0.3 m tall and 0.16–0.22 m thick. Underage human remain including cranium and some ribs and sheep/goat remains including cranium and limb bones were found in the burial. The human remain exhibit clear strike marks, suggesting that M25 may be a sacrificial burial to M8.[62] Similarly, in the northwest of M8, the rectangular burial M21 is rectangular and partitioned by a stone. No human remains were found in this burial. It was inferred that M21 was another accompanying burial for M8.[62] Among unearthed artifacts, rich personal adornments included turquoise jewelry, bronze jewelry, gold earrings, bull head-like calcite adornment, sodium calcium glass bead and agate bead (Figure S15). Other tomb contents include sheep/goat head, sheep/goat limb bone, iron sword, iron stirrup, iron hoop, copper pan, copper plate, copper spoon, utilitarian wooden and ceramic objects, leather, Chinese silk and Chinese Kaiyuan Tongbao (Tang) coins. Since skeletal preservation was highly variable across these burials, we selected 6 well-preserved individuals M8、M9、M10、M14、M17 and M18 for genomic sequencing.

Wooden outer coffin tomb: the Dulan burials feature 3 wooden outer coffin tombs mostly made from local Qilian Juniper (*Sabina przewalskii* Kom.) wood. Burial M16 consists of tomb pit, timber and coffin compartment (Figure S16). The coffin compartment's floor plan is rectangular, measuring 1.86 m from east to west, 1.36 m from north to south and 1.44 m height. The inner wall of the coffin compartment is paved with wooden cube-blocks with ink markings in Tibetan indicating burial orientation and number. Under the coffin plank, we find plant seeds and grains – these are thought to indicate some connection with the Bon religion during Tubo period.[63] Moreover, a mummified human remains in M16 (Figure S17) follows an embalming method for the dead commonly found in the Tubo Empire.[61] In addition to the objects mentioned above, we have artifacts with ink markings in Tibetan, including oracle bone, cypress cube-blocks in the coffin compartment, and wooden slips. Furthermore, other tomb contents include antler

objects, amber pendant, shell ornament and some lacquerwares. We sequenced individuals from burials M15 and M16.

Earthen pit tomb: the Dulan site contains two earthen pit tombs. Burial M20 consists of a circular stone mound consisting entirely of small rocks and an earthen burial chamber (Figure S18). From a bird's eye view, the mound is oval with 8.3 m at its maximum diameter, 6.8 m at its minimum diameter and with a surviving height of 0.46m. The chamber contains a sterile subsoil second-tier ledge on the north side that rises to 0.24 m in height. The south side of the second-tier ledge is built with stone blocks. Jumbled human remains were found above the second-tier ledge and scattered horse bones were also discovered south of this ledge. Looting had the burial posture of the human remained unclear. Remaining grave goods were few, consisting of nine iron artifacts, two bone artifacts, two leathers and several silk fabrics. In this study, we sequenced the individual from burial M20.

Brick chamber tomb: Brick chamber tombs mirror the influence of Han culture originating in the Central Plains region.[64] Only one brick chamber tomb was found at the Dulan site. Burial M19 consists of ramp (with slope), tomb pit, sealed gate and tomb chamber. The ramp, opening at the east of tomb chamber and sealed with stone, was 1.33 m long, 0.89 m wide and 2.44–2.78 m deep, running to a vertical earthen pit. The floor plan of the chamber was approximately quadrilateral and ten circular juniper columns of 3.3 m length and 0.33 m diameter covering the top of chamber (Figure S19). The tips of the juniper columns were covered up with gravel. The chamber wall was constructed using square bricks and ran to a height of 1.89 m and thickness of 0.28 m. The tomb chamber floor was also covered by gravel. Looting had damaged the burial receptacle, and only sporadic wood fragments could indicate the presence of a wooden coffin. Only five pottery sherds, one iron nail and one leather piece were discovered. On the whole, the burial style and construction material bore a strong resemblance to Tang Dynasty Tombs.[64] We sequenced the individual from burial M19.

In addition to 25 burials, 5 sacrificial horse pits were found at the Dulan site. These horse pits were elongated, strip-shaped and all located near the large or medium stone chamber tombs. Pits K1 and K2 were the best-preserved. K1 consisted of stone frame and earthen pit (Figure S20). The pit was 4.28 m long, 0.78–0.89 m wide and 1.61–1.78 deep. Five fully intact mare skeletons aged >13 years at time of death, were discovered in its pit. Pit K2 was also rectangular, 14.92 m in length, 1.12–1.28 m in width and 0.4–1.48 m thick. The pit contained 9 complete stallion remains, aged >5 years at time of death. All stallions were oriented westwards and bore clear strike marks on their skulls. In general, such a sacrificial custom is popular on Tibetan Plateau during Tubo period.[61]

Overall, based on burial style and custom, the Dulan site exhibits typical Tubo style burial characteristics. Firstly, in terms of burial layout, the largest burials are located centrally and are orbited by smaller burials. Secondly, despite severe destruction of mounds, the stone chamber tomb with mound and the floor plan of most burials was clearly trapezoidal, akin to typical Tubo tombs in Tibetan Plateau. Thirdly, some unearthed objects with ink markings in Tibetan, such as oracle bones, wooden slip and wooden cube-blocks in the coffin compartment furnished direct evidence of Tubo influence. Fourthly, taking the perspective of burial customs, cramation burial in M4 and mummified human remain in M16 represented frequently seen Tubo forms of burial. Plant seeds and grains at M16 were heaped under the coffin plank, in a custom thought to be related to the Bon religion in Tibet. The wooden outer coffins were built with nine or seventeen layers of cube-blocks in the case M16 and M23, in another nod to ancient Tibetan burial custom and hierarchy. Sacrificial customs were also popular in Tibetan Plateau during Tubo period. On the other hand, a Chinese Kaiyuan Tongbao coin, silk fabrics and the structure style of brick chamber tomb all reflect Han influence from the Central Plains, while the artifacts like Dragonfly-eye glass beads and turquoise jewelry mirror the cultural exchanges with ancient Western Regions along the Silk Road.

Radiocarbon dating of sample materials

A total of 10 human bone samples were analyzed by accelerator mass spectrometry (AMS) at Lanzhou University in Lanzhou, China. Uncalibrated direct carbon dates were successfully obtained for 10 bone samples (Table S1). The resulting ^{14}C dates were calibrated using OxCal v4.4[46] and the IntCal20 calibration curve.[65]

METHOD DETAILS

Ancient DNA extraction and library preparation

We extracted DNA from 10 samples in a dedicated aDNA facility at Fudan University, following established precautions for working with ancient human DNA.[66,67] Human remains were surface-cleaned and ground to a fine powder. We used 100 mg of bone powder to extract DNA. The prelysis step included the addition of 1 mL extraction buffer, containing 0.5 M EDTA, 0.25 mg/mL Proteinase K (Merck, Germany), pH 8.0, followed by 1 h rotation at 37°C. After centrifugation, the supernatant was discarded, and 2.5 mL extraction buffer was added followed by overnight rotation at 37°C. We mixed 20 μL magnetic beads (Enlighten Biotech, China) with 12.5 mL binding buffer containing 5 M Guanidine hydrochloride, 40% Isopropanol, 25 mM sodium acetate, 0.05% Tween-20 (Sigma Aldrich, Germany), pH 5.2. Then, we transferred the supernatant (~2.5 mL) to a binding buffer/bead mixture followed by an extraction using a robot (Enlighten Biotech, China) procedure.[66] Finally, the DNA was eluted with 50 μL TET buffer (QIAGEN, Germany). We prepared double-stranded libraries following Meyer's protocols,[68] but with minor modifications outlined below.[69,70] The end-repair step was performed in 25 μL reactions using 20 μL of DNA extract. This was incubated for 20 min at 12°C and 15 min at 37°C, purified using a standard MinElute (Qiagen, Germany) purification step and eluted in 15 μL TET (Qiagen, Germany). Next, Illumina-specific adapters were ligated to the end-repaired DNA in 25 μL reactions. The reaction was incubated for 15 min at 20°C and purified with another MinElute purification step before being eluted in 20 μL EB Buffer (Qiagen, Germany). The adapter fill-in reaction was performed in a final volume of 25 μL and incubated for 20 min at 37°C followed by 20 min at 80°C to inactivate the Bst enzyme (NEB, USA). Libraries were amplified with indexing primers in two parallel PCRs using Q5 High-Fidelity DNA Polymerase (NEB, USA). We purified indexed products using the AMPure XP bead (Beckman Coulter, USA). We qualified the clean-up libraries using Qubit 2.0 (Thermo Fisher, USA). We converted the libraries into circular single-strand libraries adapted to the MGISEQ-2000 instrument,[66] using the MGI Easy Universal Library Conversion Kit (App-A, Cat. No.: 1000004155). Finally, we made DNBs and sequenced the libraries with the MGISEQ-2000RS High-throughput (Rapid) Sequencing Kit (App-A, PE100, Cat. No.: 1000005662).

QUANTIFICATION AND STATISTICAL ANALYSIS

Sequence data processing

We trimmed the sequencing adapters and merged the paired-end reads into one sequence using AdapterRemoval v2.3.1.[54] We then mapped the merged reads onto the human reference genome (hs37d5; GRCh37 with decoy sequences) using BWA v0.7.17[66] samse and parameters -l 1024 and -n 0.01. Dedup v0.12.3[67] was used to remove the PCR duplicates. Then, we clipped four bases from both ends of each read to avoid excess C->T and G- > A transitions at the ends of the sequences, using trimBam implemented in BamUtil v1.0.14 (https://github.com/statgen/bamUtil). We filtered the alignment quality using mpileup implemented in samtools by using parameters -q30, -Q30, then generated pseudo-haploid calls for each sample by using the 1240k dataset as reference and parameter –RandomHaploid in pileupCaller software (https://github.com/stschiff/sequenceTools).

Authentication of ancient DNA

MapDamage2.0[27] was used to detect the post-mortem pattern of ancient DNA and to estimate 5′ C>T misincorporation rates. We then used Schmutzi v1.5.5.5 to obtain the consensus sequences of mitochondrial genome.[29] The mitochondrial contamination rates were estimated from haplogroup defining mutations following the method described in Sun et al.[71] We also estimated the nuclear genome contamination rate in all samples, using the assigned male sample ANGSD v0.931.[30]

Genetic sexing and uniparental haplogroup assignment

Two methods were used to assign the genetic gender to our samples.[72,73] We used the log2fasta program implemented in Schmutzi to call the mtDNA consensus sequences. Then, mitochondrial haplogroups were assigned using Haplogrep2.[57] Mutations that appeared when checked against rCRS were also re-checked in BAM (Binary Alignment Map) files through visual inspection using the IGV software.[59] Y chromosome haplogroups were examined by aligning a set of positions in the ISOGG (International Society of Genetic Genealogy, http://isogg.org/) and Y-full (https://www.yfull.com/tree/) databases, in which we only restrict our analysis to reads with base and mapping quality higher than 30. Haplogroup determination was performed with the script Yleaf.py in Yleaf software,[58] which provides outputs for allele counts of ancestral

and derived SNPs along a path of branches of the Y-chromosome tree. Finally, we re-checked the SNPs by visual inspection with IGV software.[59]

Kinship detection

We used lcMLkin[28] software to detect the genetic kinship between ancient individuals. No pair of individuals closer than second-degree was detected.

Data merging

We merged our data with two previously published datasets using mergeit from EIGENSOFT,[39] one based on Illumina array 1240k dataset which includes 1,233,013 SNPs, and the other based on Affymetrix Human Origins array which includes 597,573 SNPs.[15,23,31–38] The Human Origin dataset was used in analyses that involved modern populations including smartpca, ADMIXTURE, and *f-statistics*-based analyses for modern Tibetan,[34] while the 1240k dataset was used in all other analyses for ancient individuals.

Principal components analysis

PCA analysis was performed using smartpca v16000 implemented in EIGENSOFT on the Human Origin dataset. We used the default parameters and set lsqproject to YES.[39] The modern populations were used to calculate the principal components (PCs), and then the ancient samples were projected onto the top two components.

ADMIXTURE analysis

ADMIXTURE v1.3.0[60] was used to perform an unsupervised admixture analysis. After pruning for linkage disequilibrium in plink v1.90[74] using parameter parameters –indep-pairwise 200 25 0.4,[75,76] ADMIXTURE was run with five-fold cross-validation and 100 bootstrap replicates and varies of ancestral populations K ranging from 2 to 14.

f-statistics

QpDstat v980 was used to calculate the f_4-statistics using parameter f_4-mode: YES.[31,75] *Qp3Pop* v651 was used to calculate the outgroup-f_3 and admixture-f_3 using parameter inbreed: YES. Both software are implemented in ADMIXTOOLS.

qpWave analysis

Q*pWave* v600 implemented in ADMIXTOOLS was used to test whether pairs of populations were genetically homogenous to a set of outgroups[31] using parameter allsnps: YES and inbreed YES.

Admixture modelling

We used *qpAdm*, f_4-ratio and *qpGraph* implemented in ADMIXTOOLS to estimate the ancestries proportion in our samples. Q*pAdm* v810 was used to estimate the admixture proportion of a target population as the combination of the source populations[77] using parameters allsnps: YES and inbreed: YES. In this study, we used two strategies for the analyses, the first using the combination method where we separated our potential sources to several groups and modelled our target as the combination of one to three potential sources from different groups. And the second using the rotation method, which was well described in Harney et al.[78,79] Briefly, we used a set of distantly related outgroup as fixed outgroup and added the population to the outgroup when a source population is not be chosen as a potential source. *F4*-ratio v0.1[31] was used to estimate the proportion of Upper_YR_LN ancestry in the target populations and qpGraph[39,42] was used to reconstruct the deep population history of target population which combined the result of f_2, f_3 and f_4-statistics. The worst Z-scores smaller than 3 indicates a fitted model.